Title

PTPRG inhibition by DNA methylation and cooperation with RAS gene activation in childhood acute lymphoblastic leukemia

Journal

International Journal of Cancer, 135(5)

ISSN

0020-7136

Authors

Xiao, Jianqiao
Lee, Seung-Tae
Xiao, Yuanyuan
et al.

Publication Date

2014-09-01

DOI

10.1002/ijc.28759

Peer reviewed

HHS Public Access

Author manuscript

Int J Cancer. Author manuscript; available in PMC 2016 March 03.

Published in final edited form as:

Int J Cancer. 2014 September 1; 135(5): 1101–1109. doi:10.1002/ijc.28759.

PTPRG inhibition By DNA methylation and cooperation with *RAS* gene activation in childhood acute lymphoblastic leukemia

Jianqiao Xiao[1], **Seung-Tae Lee**[1,2], **Yuanyuan Xiao**[1], **Xiaomei Ma**[3], **E. Andres Houseman**[4], **Ling-I Hsu**[5], **Ritu Roy**[6], **Margaret Wrensch**[7], **Adam J. de Smith**[1], **Anand Chokkalingam**[5], **Patricia Buffler**[5], **John K. Wiencke**[7], and **Joseph L. Wiemels**[1,*]

[1]Department of Epidemiology and Biostatistics, University of California San Francisco, San Francisco CA 94158

[2]Department of Laboratory Medicine & Genetics, Samsung Medical Center, Sungkyunkwan University School of Medicine, Seoul, Korea

[3]Department of Epidemiology and Public Health, Yale University, New Haven, CT 06520

[4]College of Public Health and Human Sciences, Oregon State University, Corvallis, OR 97331

[5]Division of Epidemiology, School of Public Health, University of California Berkeley, Berkeley CA 94720

[6]Cancer Center Institute, University of California San Francisco, San Francisco CA 94158

[7]Department of Neurological Surgery, University of California San Francisco, San Francisco CA 94158

Abstract

While the cytogenetic and genetic characteristics of childhood acute lymphoblastic leukemias (ALL) are well studied, less clearly understood are the contributing epigenetic mechanisms that influence the leukemia phenotype. Our previous studies and others identified gene mutation (*RAS*) and DNA methylation (*FHIT*) to be associated with the most common cytogenetic subgroup of childhood ALL, high hyperdiploidy (having 5 more chromosomes). We screened DNA methylation profiles, using a genome-wide high dimension platform, of 166 childhood ALLs and 6 normal pre-B cell samples and observed a strong association of DNA methylation status at the *PTPRG* locus in human samples with levels of *PTPRG* gene expression as well as with *RAS* gene mutation status. In the 293 cell line, we found that *PTPRG* expression induces de-phosphorylation of ERK, a downstream RAS target which may be critical for mutant RAS-induced cell growth. In addition, *PTPRG* expression is up-regulated by RAS activation under DNA hypomethylating conditions. An element within the *PTPRG* promoter is bound by the RAS-responsive transcription factor RREB1, also under hypomethylating conditions. In conclusion, we provide evidence that DNA methylation of the *PTPRG* gene is a complementary event in oncogenesis induced by *RAS* mutations. Evidence for additional roles for PTPR family member genes is also suggested. This

To whom correspondence should be addressed: tel +1 (415) 514-0577; fax +1 (415) 502-7411; joe.wiemels@ucsf.edu.

Conflict of interest statement: None declared

provides a potential therapeutic target for *RAS*-related leukemias as well as insight into childhood ALL etiology and pathophysiology.

Keywords

childhood acute lymphoblastic leukemia; RAS; PTPRG; DNA methylation

Introduction

The *RAS* oncogenes *NRAS* and *KRAS* are commonly activated by mutation in both acute lymphoid and myeloid leukemias of children and in up to 40% of high hyperdiploid leukemias (>50 chromosomes in karyotype), suggesting a phenotypic complement to high hyperdiploidy in producing the leukemic phenotype [1, 2]. Up-regulation of RAS signal transduction pathways contribute to the leukemic phenotype in animal models and human disease, and the *RAS* pathway has been utilized as a therapeutic target for hematologic malignancies [3–5]. The formation of hyperdiploidy is known to be a prenatal event in leukemogenesis [6–9], with *RAS* mutation being postnatal [2]. Understanding cooperating epigenetic events in *RAS*-induced leukemogenesis will reveal additional details about etiology of the disease and additional therapeutic targets.

We previously noted a strong association between DNA methylation and reduced expression of the tumor suppressor gene *FHIT* and childhood ALL with high hyperdiploidy (51–68 chromosomes in karyotype, referred to as “hyperdiploidy” from here on) [10]. The association between DNA methylation of *FHIT* and the hyperdiploid phenotype was replicated in another study [11] and also extended to myeloid lymphoblastic leukemias [12]. In the current study we explored whether this association is a dominant feature in hyperdiploid leukemia by comparing its strength of association relative to genes and CpG loci across the genome. High dimension CpG array analysis indicated that DNA methylation of *PTPRG* (a gene neighboring *FHIT* at chromosome 3p14.2, and encoding a receptor-type protein phosphatase) was more strongly associated with *RAS* mutation status, as well as hyperdiploidy, compared to *FHIT* DNA methylation status. These genes, while located over 300,000 nucleotides apart, are situated in reverse orientation and likely co-regulated to some degree. In the current study, we report genetic association and functional analyses to demonstrate a link between the RAS signaling pathway and PTPRG function, a likely primary target for DNA methylation control in leukemogenesis in cooperation with RAS pathway mutation, as well as considering the role of the rest of the 19-member receptor-type PTP gene family.

Materials and Methods

Clinical samples, cell lines, plasmids, and DNA/RNA extractions

Bone marrow DNA from children with pre-B cell ALL was obtained from the California Childhood Leukemia Study and comprised the same population used previously in studies of *KRAS* and *NRAS* gene mutations [2]. All participants supplied written consent and the study was reviewed and approved by the UC Berkeley Institutional Review Board. A set of 166 of

pre-B ALL with *RAS* mutation (*KRAS* and/or *NRAS*) characterization and cytogenetic classifications were chosen for DNA methylation analysis using the higher density Illumina HM450K array analysis. Refinement and validation of these same samples was performed with Sequenom DNA methylation analysis. Among these cases, 34 had *RAS* mutations and 38 were high hyperdiploid (Supplementary Table 1). Light density purified leukemic bone marrow cells (1×10^7 cells) exhibiting greater than 80% blasts prior to purification were isolated into DNA and RNA using AllPrep (Qiagen). DNA and RNA from bone marrow mononuclear cells were extracted using Qiagen's AllPrep DNA/RNA/Protein Mini Kit.

The cell line HEK-293 (ATCC, Manassas, Virginia) was maintained in Dulbecco's Modified Eagle Medium with 10% fetal bovine serum (FBS) (Hyclone, Logan, Utah) and cell line 697 (ATCC) were maintained in RPMI 1640 supplemented with 10% FBS. Plasmids containing the wild type (wt) *KRAS* gene, pMSCV/RAS Wt, and plasmids containing the mutant *KRAS* gene, pMSCV/RAS Mut G12D were kindly provided by Dr. Benjamin Braun (UCSF). The pGL4.23[luc2/minP] plasmid containing the luciferase reporter gene was purchased from Promega (Madison, Wisconsin). Plasmid DNAs were extracted using Qiagen's Mini-Prep or Midi-Prep plasmid DNA purification kits (Qiagen, Valencia, California). DNA from normal human fetal bone marrow was obtained from aborted fetuses; pre-B-cells were isolated with flow sorting as lin-, CD34+, CD19+, CD10+ cells as described [13]. Samples were obtained under the approval and supervision of the UCSF Committee on Human Research.

DNA methylation analysis

DNA samples were treated with bisulfite to convert unmethylated cytosines to uracil using the EZ DNA methylation kit (Zymo Research, Irvine, California) according to the cycling protocol (16 cycles: 95°C, 30 seconds and 50°C, 60). The bisulfite-treated DNA was amplified and hybridized onto the Illumina HumanMethylation450 Beadchip (HM450K, n = 166, Illumina, San Diego, CA) according to the manufacturer's specifications. This array allows a genome-wide interrogation of 485,764 CpG sites for more than 32,000 transcripts. Raw data was processed using the GenomeStudio software (Illumina), and the average methylation values (β) ranging from 0 (fully hypomethylated) to 1 (fully hypermethylated) were identified for each probe. Before analyzing the methylation data, we excluded possible sources of technical errors according to the following quality control metrics. CpG sites with detection *P* values > 1.0×10^{-4} were removed from analysis. Methylation samples with a high proportion (>4%) of suboptimal data (n = 2) were eliminated from analysis. Additionally, probes which contained polymorphic SNPs (N = 89,677), and those on the X-chromosome (n = 11,645) were excluded. Data was normalized for array and array position using linear mixture model, adjusting for chip and array position effects.

As an additional confirmation/validation analysis, a Sequenom MassARRAY quantitative methylation analysis using the MassARRAY Compact System (Sequenom, San Diego, California) was performed for single gene (*PTPRG*) on the same 166 samples used for the Illumina HM450K analysis. Part of the promoter region of *PTPRG* containing the CpG island [chromosome 3, 61522065-61522387 (Hg18)] was amplified by PCR using methylation specific primers designed with the Epidesigner software (Sequenom)

(Supplementary Table 2). A subset of the leukemia cell samples which were also assayed with HM450K (n = 81) with good quality RNA (by Agilent Bioanalyzer results) was subjected to expression array analysis using Nugen Ovation RNA labeling and Affymetrix 1.0 ST microarray. Thirty-three of the 81 were hyperdiploid; 14 of these hyperdiploid were *RAS*-mutant (5 *NRAS* and 9 *KRAS*). Of the non-hyperdiploids, there were 3 *NRAS* and 5 *KRAS* mutant, for a total of 22 *RAS* mutations. The leukemia samples for DNA expression analysis are a subset of the same set of subjects used for the initial screening by HM450K and Sequenom.

Statistical analysis

Statistical analysis and data visualization was carried out using the *R* statistical software with Bioconductor packages. DNA methylation levels from the Illumina arrays were transformed by arcsin(sqroot) for variance stabilization. Methylation or expression levels between two groups were compared using the moderated *t*-statistics and a mixed effect model to accommodate correlations between samples from the same donor. The *qvalue* package in R was used to correct for multiple comparisons (*Q* values).

Gene-level DNA methylation analysis was performed using a script that grouped CpG sites annotated within the same gene region/feature, using Illumina's annotation data. Gene regions were ranked for association with *RAS* status using the median P-value for CpG sites within a region (for those regions represented by more than one CpG site).

Cloning of the *PTPRG* cDNA and promoter fragments

The full length human *PTPRG* cDNA protein coding region was obtained by reverse transcriptase PCR as follows: Total RNAs were extracted from the leukemia cell line, 697 using the Qiagen Allprep kit; 5 μg total RNA was used to synthesize the first strand of cDNA using Superscript II (Invitrogen, Grand Island, New York) and the gene specific primer PTPRG-R (Supplementary Table 2) according to the manufacturer's protocol; 2 μl of the newly synthesized cDNAs were then used as template to amplify the full length protein coding region of the *PTPRG* cDNA using primer PTPRG-F and PTPRG-R-flag (Supplementary Table 2). PCR reactions were performed using iProof High-Fidelity DNA polymerase (Bio-Rad, Hercules, California) for 30 cycles of 98°C for 10 seconds, and 66°C for 5 min, after an initial denaturation of 1 min at 98°C. The PCR products were first sequenced to confirm amplification of the correct *PTPRG* sequence and then cloned into pMSCVneo plasmid (Clontech, Mountain View, California) between *Eco*RI and *Bgl*II sites. The plasmid expressing the human *PTPRG* gene was designated pMSCV/PTPRG. Expression of the *PTPRG* gene was confirmed by Western blotting using a Rabbit anti-PTPRG polyclonal antibody (Sigma-Aldrich, St. Louis, Missouri) in total cellular proteins harvested from 293 cells transfected with the *PTPRG* clone (data not shown). Five fragments of the *PTPRG* promoter region were amplified by PCR using specific primers (Supplementary Table 2). To mutate the putative RAS responsive element (RRE) in fragment C (see Results and Figure 4), the putative RRE sequence, ccccaaactgtccca, was replaced by tgactcgaattcaca, a scrambled sequence containing an *Eco*RI restriction site. Two separate PCRs were performed: primers PTPRG-prmt-F1 and ptp-mutRRE-R were used to amplify the region upstream of the putative RRE, and primers ptp-mutRRE-F and PTPRG-

prmt-R2 were used to amplify the region downstream of the putative RRE. After restriction digestion with *EcoR*I and ligation of the two PCR fragments, the full fragment C was then reamplified with primers PTPRG-prmt-F1 and PTPRG-prmt-R2. The PCR products for all five fragments were then cloned into plasmid pGL4 23[luc/minP] (Promega, Madison, WI) between the *Kpn*I and *Hind*III restriction sites upstream of the luciferase reporter gene. The sequence of cloned fragments were then confirmed by restriction digestion and sequencing (data not shown).

DNA transfection and Luciferase assays

Plasmid DNA was transfected into cell line 293 (ATCC, Manassas, VA) using LipofectAmine 2000 according to the manufacturer's protocol. Total cellular proteins were harvested 24 h after transfection. The Steady-Glo® Luciferase Assay System (Promega) was used to detect luciferase activity of cells transfected with plasmids encoding the luciferase gene. Luciferase activity was detected using the Bio-Tek luminometer (Bio-Tek Instruments, Winooski, VT).

Chromatin immunoprecipitation (ChIP) was performed using 697 cells grown in their log phase, anti-RREB1 antibody (Santa Cruz Biotechnology, cat# sc-138055), and the EZ-ChIP™ Chromatin Immunoprecipitation Kit (Millipore, Cat# 17-371), according to the protocol provided by the manufacturer. The promoter region of *PTPRG* containing the putative RRE was amplified by SYBR green real-time PCR using primers PTPRG-prmt-F4 and PTPRG-prmt-R2 (Supplementary Table 2).

Phosphoprotein detection

Five phosphorylated proteins of the Ras signal transduction pathway were detected using the Bio-Plex Phospho 5-plex Panel for detecting phosphorylated Akt, ERK1/2, IκB-α, JNK, and p38 MAPK (Bio-Rad, Hercules, CA). To detect the effects of PTPRG on tyrosine phosphorylation involved in the RAS signaling pathway, cell line 293 grown in 6 well plates were transfected with the *PTPRG* cDNA clone, with or without co-transfection of the *KRAS* Wt or *KRAS* mutant gene. Twenty-four h after transfection, cells were harvested and phosphoproteins were detected using the Bio-Plex Phospho 5-plex Panel #X70-00001RD kit according to the manufacturer's protocols.

De-methylation of genomic DNA

To induce demethylation of genomic DNA, cell line 293 (which harbor fully methylated *PTPRG* promoter) were cultured in growth medium containing 1 μM of 5-Aza-2′-Deoxycytidine (5-Aza-d-C). For normal cell controls, cells were grown in medium containing equal concentration of DMSO that was used to dissolve 5-Aza-d-C. Culture medium was changed each 24 h under the same conditions. Cells were maintained under such conditions for 72 h before, and during DNA transfections.

Quantitative Real-time RT-PCR and Western blotting

Cell line 293 (which is completely methylated at PTPRG as determined by the Sequenom assay) treated with either 5-Aza-2′-Deoxycytidine or DMSO only were transfected with either the pMSCV/neo plasmid or pMSCV/Ras Wt plasmid using LipofectAmine 2000

(Invitrogen) according to the protocol provided by the manufacturer. 24 h after transfection, cells were harvested and total RNA was extracted using the RNeasy kit (Qiagen). cDNA were synthesized from total RNA using Superscript II (Invitrogen). To detect mRNA expression of *PTPRG*, quantitative real-time RT-PCR was carried out in 10 μl of PCR mix containing Sybr Green master mix (Invitrogen), 1 μg of total cDNA, and specific primers for 40 cycles of denaturizing and annealing/extension (95 °C, 20 seconds, 65 °C, 1 min) after an initial step of denaturation at 95 °C for 5 min. The housekeeping gene glyceraldehyde-6-phosphate dehydrogenase (*GAPDH*) was used as the reference. Primer sequences are shown in Supplementary Table 2.

For Western blotting, total cellular proteins were extracted from above treated cells with RIPA buffer, 15 μg of proteins were loaded into each well of a 10% SDS PAGE gel. Protein expression of PTPRG and Actin were detected using rabbit anti-PTP Gamma and rabbit anti-actin (Sigma Aldrich) as primary antibodies and HRP-conjugated goat anti-rabbit IgG (Jackson Laboratories) as secondary antibody.

Results

Association of PTPRG gene methylation with RAS mutation and PTPRG expression

Using a childhood ALL sample set (n = 166 total) and a DNA methylation microarray [Illumina HM450K, [14]], *PTPRG* was among the most highly associated genes with *RAS* mutation with 32 CpG loci associated with *RAS* status ($P = 10^{-14}$), and also the same CpG loci associated with hyperdiploidy ($P = 10^{-12}$). At a gene region level, *PTPRG* was the second to the top gene (after *BARX2*) to be associated with *RAS* status in a positive direction (Supplementary Table 3). For both *PTPRG* and *FHIT*, associations were found in both the promoter region and gene body, with associations stronger for *PTPRG* than *FHIT*, as shown in Figure 1. The most significantly linked loci include both promoter CpGs as well as internal body CpGs, in different directions (Figure 1).

RNA was available for a subset of 166 HM450K-assayed study subjects (n = 81) for expression analysis. The two top CpG sites (cg05362669 and cg03826247) associated with *RAS* mutation subtype were among the top 5 CpG sites correlated to gene expression of *PTPRG* (Supplementary Table 4). Methylation of these two CpG sites were correlated with expression in opposite directions, the promoter CpGs (cg05362669) correlated in an inverse fashion but the internal gene body CpGs (cg03826247) generally in a positive direction (Figure 2). The top two loci relating to gene expression were chosen for further analysis: the promoter CpG site (cg05362669) was hypomethylated while the gene body CpG site (cg03826247) was hypermethylated in normal pre-B cells compared to leukemia cells (data not shown, derived from reference [13]). This indicates that the differential methylation observed in *RAS*-mutated leukemias is an active acquisition rather than a passive attribute.

Since both hyperdiploidy and *RAS* mutation were associated with *PTPRG* methylation, as well as with each other, we sought to determine whether hyperdiploidy and *RAS* were independent predictors of *PTPRG* methylation, specifically, the two top CpG sites for *RAS* mutation. As seen in Table 1, both *RAS* and hyperdiploidy are significant predictors of *PTRPG* methylation, when analyzed separately (Models 1 and 2) and together (Model 3).

The significant associations persisted after t (12:21), TEL-AML1 translocation was included in the model (Models 4 and 5) and after additional covariates, such as age at diagnosis, sex, mother's age, father's age, birth weight, gestational age, were added (detailed data not shown). In other words, both *RAS* and hyperdiploidy are independently associated with *PTPRG* methylation. To be sure, there is more promoter methylation and therefore suppression of expression when both high hyperdiploidy and/or *RAS* mutation is present. A visual representation of the DNA methylation status of probes within the whole gene, along with *FHIT*, is portrayed in Supplemental Figure 1.

To better define the region around the most significant loci, we performed a Sequenom DNA methylation assay surrounding the promoter CpGs (Illumina cg05362669) in the replication ALL patient sample set. All of the CpG units assessed in this manner were significantly more methylated in *RAS*-mutant positive subjects compared to *RAS*-wild type subjects, confirming the association apparent in the microarrays (Supplementary Figure 2).

Identification of RAS responsive element in PTPRG promoter

A transcription factor screening of the *PTPRG* promoter using Transfac Matinspector (www.genomatix.de) revealed a binding site for the ubiquitously expressed "RAS responsive element binding protein" (RREB1) in proximity to the DNA methylation hotspot described above (Figure 3A and Figure 4) as well as ½ of an RRE slightly upstream [15]. We sought to investigate the role of the *PTPRG* promoter and the RRE in its impact on *PTPRG* expression in response to *KRAS* activation. We cloned the *PTPRG* promoter fragments (which are in an unmethylated state) into a luciferase reporter vector and tested the luciferase activity of the 293 cell line after transfections of these constructs (Figure 3). The full promoter (Fig 3C, Fragment A) along with co-transfection of the Wt *KRAS* gene increased the promoter activity of the full-length promoter by five-fold (p value < 0.001), with lower activation by mutant *KRAS*. Removal of the RRE and its downstream sequences of the promoter (Fragment B) severely curtailed promoter activity of Wt *KRAS* (p value <0.0001 comparing fragment A to B, Wt *KRAS*). The full length promoter with mutant RRE showed the highest promoter activity (Fragment C); but all other constructs with the 5′ end of the promoter removed had no activity. The data indicate that the strongest KRAS response elements are located in the 5′ end of the promoter and the full-length RRE is most likely a repressive element in this cell line model. Functional evidence for RREB1 binding to the putative RRE was demonstrated using ChIP-PCR in the 697 cell line. In the presence of 5-Aza-d-C, pull-down using anti-RREB1 and anti-RNA polymerase exhibited strong binding to the PTPRG promoter, whereas in untreated cells (in this PTPRG methylated cell line), no binding was observed (Figure 5). In addition these findings suggest that the tumor suppressor gene *PTPRG* is a target of the signal transduction pathway from oncogenic *KRAS* gene.

PTPRG inhibits phosphorylation of ERK1/2 induced by mutant *KRAS*

To determine whether the tumor suppressor gene PTPRG functions through interfering with the RAS signaling pathway, we measured levels of phosphorylation of 5 important players in the RAS signaling pathway: Akt, ERK1/2, IκB-α, JNK, and p38 MAPK. As expected, the KRAS mutant increased levels of phosphorylation of all 5 proteins (data not shown); also,

the PTPRG protein somewhat reduced phosphorylation of these proteins in 293 cells after transfection (Figure 6 and data not shown). Interestingly, PTPRG significantly suppressed phosphorylation of ERK1/2 induced by the mutant RAS protein as shown in Figure 6 (p value<0.001, more significantly than the other four targets studied), indicating that PTPRG may attenuate the RAS signaling pathway by dephosphorylating ERK1/2.

Effects of DNA demethylation and *KRAS* expression on *PTPRG* expression

To determine whether *PTPRG* expression is directly inhibited by DNA methylation, and is up-regulated by KRAS when hypomethylated, we performed quantitative real-time RT-PCR and Western blotting to detect PTPRG expression in cell line 293 treated with, or without the demethylating agent, 5-Aza-d-C. Cells were transfected with the marker plasmid, pMSCV/neo, or pMSCV/Ras Wt, the plasmid expressing the wt *KRAS* gene. We found that *PTPRG* expression is increased by about 100% in cells treated with 5-Aza-d-C alone (p value < 0.01) (Fig. 5A, pMSCV and Aza-pMSCV). Interestingly, *PTPRG* expression was not affected by transfection of the *KRAS* expressing plasmid in untreated 293 cells (Fig. 5A and B), but it was greatly increased in cells treated with 5-Aza-d-C and transfected with pMSCV/Ras Wt (Fig. 5A, p value <0.01, and Fig. 5B lanes 3 and 4), indicating that DNA methylation may play a role in repressing PTPRG expression by inhibiting its response to KRAS expression.

Other PTPR members

To help determine whether PTPRG activity may be compensated or mirrored by other PTPR members, we analyzed DNA methylation and expression in our leukemia case series for 19 *PTPR* members and *SPRED1*, a RAS-pathway inhibition gene [16]. We found that several *PTPR* family members, including *PTPRT* and *PTPRB* are also DNA methylated in their promoters in the same fashion as *PTPRG* (Supplementary Figure 4), and also with the same gene expression pattern (eg., PTPR--A, -B, -D, -F, -K, and -N2, Supplementary Figure 5). Two genes with the opposite expression pattern with regards to *RAS* mutation (PTPRE and SPRED1) may compensate for loss of the other PTPR genes.

Discussion

The current study demonstrates for the first time that DNA methylation at *PTPRG* is strongly associated with *RAS* mutation in childhood all. We explored the PTPRG DNA methylation association with *RAS* mutation with functional cell culture assays. We previously found that *RAS* mutations are quite common in hyperdiploidy [about 35% prevalence compared to 10% prevalence of *RAS* mutations in non-hyperdiploidy patients [1, 2]], and it is possible that *RAS* pathway activation is a common feature of hyperdiploid patients even without *RAS* mutations as exemplified by their higher frequency of *FLT3* mutations [17] and *PTPN11* mutations [18], compared to other ALL subtypes. Like these genetic mutations which have postnatal origin,[2, 17] *PTPRG* methylation is likely to occur after birth and secondary to chromosomal mutations which typically have a prenatal origin [7, 9, 19]. Our previous observation that *FHIT* gene methylation was highly associated with hyperdiploidy [10] was replicated here, but the stronger associations with *PTPRG* as well as relevant functional pathway analysis indicates that the likely target for DNA methylation

in this genomic region is *PTPRG* rather than *FHIT*. The genes while located adjacent to each other are oriented in opposite directions, with promoter regions juxtaposed. A similar DNA methylation and expression pattern of other *PTPR* members as *PTPRG* additionally support the argument that PTPR function is the critical target here. PTPRG was also identified as a significant gene in the leukemia phenotype in one additional recent analysis [20], and a tumor suppressor gene in other contexts [21–23]. A limitation of the current analysis is a lack of experiments to prove *PTPRG* methylation would be actively acquired in a background of *RAS* mutation. Further functional experiments to establish the acquisition of *PTPRG* methylation in the presence of *RAS* mutation and other genetic events should be performed in engineered animal models and of leukemia and signal transduction experiments in culture. Additionally, the potential compensatory or concordant role of other PTPR members besides PTPRG was suggested by our DNA methylation and expression data, and may also be investigated in appropriate models of leukemogenesis.

RAS activation by mutation was coupled with promoter methylation and suppression of expression of *PTPRG* (Figure 1 and 2). The specific targets of PTPRG have not yet been described in hematopoietic cells, but our functional analysis suggests that ERK may reside downstream of such targets. A similar result was previously shown with PTPRG in breast cancer cells [22]. These results imply that reactivation of PTPRG in RAS-pathway activated tumors may impact the leukemic phenotype; possibly through release of DNA methylation of the *PTPRG* promoter, which may explain some of the biological activity of DNA methylation-modifying drugs. PTPRG was recently described as binding and dephosphorylating β–catenin, suggesting additional signal transduction roles along the Wnt and PI3/AKT pathways [24]. Assessing *RAS* mutation status in therapeutic studies of epigenetic modifiers could extend our observations for clinical relevance. The recent identification of another receptor-type protein phosphatase PTPRJ as an antagonist to FLT3 activation is directly parallel to our findings in the current manuscript [25]. PTPRJ is inactivated by an alternative mechanism, however (by oxidation induced by FLT3 signaling) which may also occur in RAS activated tumors since high levels of reactive oxygen species are created by RAS activation as well [26, 27]. Another membrane phosphatase, *PTPRC*, more commonly referred to as *CD45*, is frequently inactivated by point mutations in T-cell leukemia and is associated with activation of several signal transduction pathways including JAK2 [28]. Clearly, a parallel tumor suppressor paradigm for receptor-type PTP proteins is becoming commonplace in several hematopoietic malignancies.

PTPRG was identified as an obligatory factor in hematopoietic cell differentiation, as suppression of *PTPRG* expression completely abrogated hematopoietic colony formation from embryo stem cells [29]. *PTPRG* appears to be critical in megakaryocyte differentiation as well as dendritic cell and mast cell function [30, 31], and appears to have tumor suppression activity in chronic myeloid leukemia, immediately downstream (and directly binding to) the BCR-ABL1 oncogene [32]. The mechanism for expression abrogation in chronic myeloid leukemia as well as other cancer sites such as lung and colon was DNA methylation related, similar to the current report [21, 33].

In conclusion, our study implicates *PTPRG* and potentially other receptor-type PTP as a tumor suppressor in RAS-activated tumors using both primary patient evidence and *in vitro*

experiments, which has etiologic and clinical implications. The success of cancer therapeutics which rescue gene expression from aberrantly methylated promoters may rest in part from the re-expression of *PTPRG*, and mechanisms that specifically impact this process may have etiologic and clinical implications for childhood ALL as it does for other cancers in which DNA methylation of *PTPRG* and other *PTPRs* has an oncogenic impact.

Supplementary Material

Refer to Web version on PubMed Central for supplementary material.

Acknowledgments

Funding

This work was supported by NIEHS/EPA P01ES018172 (J.L.W. and P. Buffler), NCI R01CA155461 (J.L.W and X. Ma), TRDRP (18CA-0127, J.L.W.), and Leukemia and Lymphoma Society (6026-10, J.L.W.). The content is solely the responsibility of the authors and does not necessarily represent the official views of any of the funding bodies.

This research could not have been conducted without the important support from our clinical collaborators and participating hospitals, which include: University of California Davis Medical Center (Dr. Jonathan Ducore), University of California San Francisco (Dr. Mignon Loh and Dr. Katherine Matthay), Children's Hospital of Central California (Dr. Vonda Crouse), Lucile Packard Children's Hospital (Dr. Gary Dahl), Children's Hospital Oakland (Dr. James Feusner), Kaiser Permanente Sacramento (Dr. Vincent Kiley), Kaiser Permanente Santa Clara (Dr. Carolyn Russo and Dr. Alan Wong), Kaiser Permanente San Francisco (Dr. Kenneth Leung), and Kaiser Permanente Oakland (Dr. Stacy Month), and the families of the study participants. We also wish to acknowledge the effort and dedication of all our collaborators at the Northern California Childhood Leukemia Study who helped make this study possible, and the staff at the Battelle Memorial Institute, Columbus, OH who performed laboratory analyses. This work was financially supported by National Institute of Environmental Health Sciences, Grants R01 ES09137 and P42-ES04705; the Intramural Research Program of the National Cancer Institute (subcontracts 7590-S-04, 7590-S-01); the National Cancer Institute (contract N02-CP-11015), and from the National Institutes of Health. The content is solely the responsibility of the authors and does not necessarily represent the official views of the National Institute of Environmental Health Sciences or the National Cancer Institute. We mourn the unexpected passing of Patricia Buffler on September 27, 2013, Her leadership of the CCLS helped to make this study possible.

References

1. Wiemels JL, Zhang Y, Chang J, Zheng S, Metayer C, Zhang L, Smith MT, Ma X, Selvin S, Buffler PA, Wiencke JK. RAS mutation is associated with hyperdiploidy and parental characteristics in pediatric acute lymphoblastic leukemia. Leukemia. 2005; 19:415–19. [PubMed: 15674422]
2. Wiemels JL, Kang M, Chang JS, Zheng L, Kouyoumji C, Zhang L, Smith MT, Scelo G, Metayer C, Buffler P, Wiencke JK. Backtracking RAS mutations in high hyperdiploid childhood acute lymphoblastic leukemia. Blood Cells Mol Dis. 2010; 45:186–91. [PubMed: 20688547]
3. Braun BS, Tuveson DA, Kong N, Le DT, Kogan SC, Rozmus J, Le Beau MM, Jacks TE, Shannon KM. Somatic activation of oncogenic KRAS in hematopoietic cells initiates a rapidly fatal myeloproliferative disorder. Proc Natl Acad Sci U S A. 2004; 101:597–602. [PubMed: 14699048]
4. Lauchle JO, Kim D, Le DT, Akagi K, Crone M, Krisman K, Warner K, Bonifas JM, Li Q, Coakley KM, Diaz-Flores E, Gorman M, et al. Response and resistance to MEK inhibition in leukaemias initiated by hyperactive Ras. Nature. 2009; 461:411–4. [PubMed: 19727076]
5. Zhang J, Mullighan CG, Harvey RC, Wu G, Chen X, Edmonson M, Buetow KH, Carroll WL, Chen IM, Devidas M, Gerhard DS, Loh ML, et al. Key pathways are frequently mutated in high-risk childhood acute lymphoblastic leukemia: a report from the Children's Oncology Group. Blood. 2011; 118:3080–7. [PubMed: 21680795]
6. Maia AT, Tussiwand R, Cazzaniga G, Rebulla P, Colman S, Biondi A, Greaves M. Identification of preleukemic precursors of hyperdiploid acute lymphoblastic leukemia in cord blood. Genes Chromosomes Cancer. 2004; 40:38–43. [PubMed: 15034866]

7. Panzer-Grumayer ER, Fasching K, Panzer S, Hettinger K, Schmitt K, Stockler-Ipsiroglu S, Haas OA. Nondisjunction of chromosomes leading to hyperdiploid childhood B-cell precursor acute lymphoblastic leukemia is an early event during leukemogenesis. Blood. 2002; 100:347–9. [PubMed: 12070048]

8. Yagi T, Hibi S, Tabata Y, Kuriyama K, Teramura T, Hashida T, Shimizu Y, Takimoto T, Todo S, Sawada T, Imashuku S. Detection of clonotypic IGH and TCR rearrangements in the neonatal blood spots of infants and children with B-cell precursor acute lymphoblastic leukemia. Blood. 2000; 96:264–8. [PubMed: 10891460]

9. Gruhn B, Taub JW, Ge Y, Beck JF, Zell R, Hafer R, Hermann FH, Debatin KM, Steinbach D. Prenatal origin of childhood acute lymphoblastic leukemia, association with birth weight and hyperdiploidy. Leukemia. 2008; 22:1692–7. [PubMed: 18548099]

10. Zheng S, Ma X, Zhang L, Gunn L, Smith MT, Wiemels JL, Leung K, Buffler PA, Wiencke JK. Hypermethylation of the 5′ CpG Island of the FHIT Gene Is Associated with Hyperdiploid and Translocation Negative Subtypes of Pediatric Leukemia. Cancer Res. 2004; 64:2000–6. [PubMed: 15026336]

11. Paulsson K, An Q, Moorman AV, Parker H, Molloy G, Davies T, Griffiths M, Ross FM, Irving J, Harrison CJ, Young BD, Strefford JC. Methylation of tumour suppressor gene promoters in the presence and absence of transcriptional silencing in high hyperdiploid acute lymphoblastic leukaemia. Br J Haematol. 2009; 144:838–47. [PubMed: 19120349]

12. Stam RW, den Boer ML, Passier MM, Janka-Schaub GE, Sallan SE, Armstrong SA, Pieters R. Silencing of the tumor suppressor gene FHIT is highly characteristic for MLL gene rearranged infant acute lymphoblastic leukemia. Leukemia. 2006; 20:264–71. [PubMed: 16357833]

13. Lee ST, Xiao Y, Muench MO, Xiao J, Fomin ME, Wiencke JK, Zheng S, Dou X, de Smith A, Chokkalingam A, Buffler P, Ma X, et al. A global DNA methylation and gene expression analysis of early human B-cell development reveals a demethylation signature and transcription factor network. Nucleic Acids Res. 2012; 40:11339–51. [PubMed: 23074194]

14. Bibikova M, Barnes B, Tsan C, Ho V, Klotzle B, Le JM, Delano D, Zhang L, Schroth GP, Gunderson KL, Fan JB, Shen R. High density DNA methylation array with single CpG site resolution. Genomics. 2011; 98:288–95. [PubMed: 21839163]

15. Thiagalingam A, De Bustros A, Borges M, Jasti R, Compton D, Diamond L, Mabry M, Ball DW, Baylin SB, Nelkin BD. RREB-1, a novel zinc finger protein, is involved in the differentiation response to Ras in human medullary thyroid carcinomas. Mol Cell Biol. 1996; 16:5335–45. [PubMed: 8816445]

16. Stowe IB, Mercado EL, Stowe TR, Bell EL, Oses-Prieto JA, Hernandez H, Burlingame AL, McCormick F. A shared molecular mechanism underlies the human rasopathies Legius syndrome and Neurofibromatosis-1. Genes Dev. 2012; 26:1421–6. [PubMed: 22751498]

17. Chang P, Kang M, Xiao A, Chang J, Feusner J, Buffler P, Wiemels J. FLT3 mutation incidence and timing of origin in a population case series of pediatric leukemia. BMC Cancer. 2010; 10:513. [PubMed: 20875128]

18. Molteni CG, Te Kronnie G, Bicciato S, Villa T, Tartaglia M, Basso G, Biondi A, Cazzaniga G. PTPN11 mutations in childhood acute lymphoblastic leukemia occur as a secondary event associated with high hyperdiploidy. Leukemia. 2010; 24:232–5. [PubMed: 19776760]

19. Wiemels J. Chromosomal translocations in childhood leukemia: natural history, mechanisms, and epidemiology. J Natl Cancer Inst Monogr. 2008:87–90. [PubMed: 18648011]

20. Wong NC, Ashley D, Chatterton Z, Parkinson-Bates M, Ng HK, Halemba MS, Kowalczyk A, Bedo J, Wang Q, Bell K, Algar E, Craig JM, et al. A distinct DNA methylation signature defines pediatric pre-B cell acute lymphoblastic leukemia. Epigenetics. 2012; 7:535–41. [PubMed: 22531296]

21. Cheung AK, Lung HL, Hung SC, Law EW, Cheng Y, Yau WL, Bangarusamy DK, Miller LD, Liu ET, Shao JY, Kou CW, Chua D, et al. Functional analysis of a cell cycle-associated, tumor-suppressive gene, protein tyrosine phosphatase receptor type G, in nasopharyngeal carcinoma. Cancer Res. 2008; 68:8137–45. [PubMed: 18829573]

22. Shu ST, Sugimoto Y, Liu S, Chang HL, Ye W, Wang LS, Huang YW, Yan P, Lin YC. Function and regulatory mechanisms of the candidate tumor suppressor receptor protein tyrosine

phosphatase gamma (PTPRG) in breast cancer cells. Anticancer Res. 2010; 30:1937–46. [PubMed: 20651337]

23. Wang Z, Shen D, Parsons DW, Bardelli A, Sager J, Szabo S, Ptak J, Silliman N, Peters BA, van der Heijden MS, Parmigiani G, Yan H, et al. Mutational analysis of the tyrosine phosphatome in colorectal cancers. Science. 2004; 304:1164–6. [PubMed: 15155950]
24. Hashemi H, Hurley M, Gibson A, Panova V, Tchetchelnitski V, Barr A, Stoker AW. Receptor tyrosine phosphatase PTPgamma is a regulator of spinal cord neurogenesis. Mol Cell Neurosci. 2011; 46:469–82. [PubMed: 21112398]
25. Godfrey R, Arora D, Bauer R, Stopp S, Muller JP, Heinrich T, Bohmer SA, Dagnell M, Schnetzke U, Scholl S, Ostman A, Bohmer FD. Cell transformation by FLT3 ITD in acute myeloid leukemia involves oxidative inactivation of the tumor suppressor protein-tyrosine phosphatase DEP-1/PTPRJ. Blood. 2012
26. Irani K, Xia Y, Zweier JL, Sollott SJ, Der CJ, Fearon ER, Sundaresan M, Finkel T, Goldschmidt-Clermont PJ. Mitogenic signaling mediated by oxidants in Ras-transformed fibroblasts. Science. 1997; 275:1649–52. [PubMed: 9054359]
27. Adachi Y, Shibai Y, Mitsushita J, Shang WH, Hirose K, Kamata T. Oncogenic Ras upregulates NADPH oxidase 1 gene expression through MEK-ERK-dependent phosphorylation of GATA-6. Oncogene. 2008; 27:4921–32. [PubMed: 18454176]
28. Porcu M, Kleppe M, Gianfelici V, Geerdens E, De Keersmaecker K, Tartaglia M, Foa R, Soulier J, Cauwelier B, Uyttebroeck A, Macintyre E, Vandenberghe P, et al. Mutation of the receptor tyrosine phosphatase PTPRC (CD45) in T-cell acute lymphoblastic leukemia. Blood. 2012
29. Sorio C, Melotti P, D'Arcangelo D, Mendrola J, Calabretta B, Croce CM, Huebner K. Receptor protein tyrosine phosphatase gamma, Ptp gamma, regulates hematopoietic differentiation. Blood. 1997; 90:49–57. [PubMed: 9207437]
30. Lissandrini D, Vermi W, Vezzalini M, Sozzani S, Facchetti F, Bellone G, Mafficini A, Gentili F, Ennas MG, Tecchio C, Sorio C. Receptor-type protein tyrosine phosphatase gamma (PTPgamma), a new identifier for myeloid dendritic cells and specialized macrophages. Blood. 2006; 108:4223–31. [PubMed: 16896153]
31. Arimura Y, Yagi J. Comprehensive expression profiles of genes for protein tyrosine phosphatases in immune cells. Sci Signal. 2010; 3:rs1. [PubMed: 20807954]
32. Della Peruta M, Martinelli G, Moratti E, Pintani D, Vezzalini M, Mafficini A, Grafone T, Iacobucci I, Soverini S, Murineddu M, Vinante F, Tecchio C, et al. Protein tyrosine phosphatase receptor type {gamma} is a functional tumor suppressor gene specifically downregulated in chronic myeloid leukemia. Cancer Res. 2010; 70:8896–906. [PubMed: 20959494]
33. van Roon EH, de Miranda NF, van Nieuwenhuizen MP, de Meijer EJ, van Puijenbroek M, Yan PS, Huang TH, van Wezel T, Morreau H, Boer JM. Tumour-specific methylation of PTPRG intron 1 locus in sporadic and Lynch syndrome colorectal cancer. Europ J Hum Genetics. 2011; 19:307–12. [PubMed: 21150880]

Novelty and Impact

This manuscript describes for the first time an epigenetic feature complement to *RAS* gene mutation in pediatric ALL – this being the epigenetic inactivation of *PTPRG*, a protein phosphatase. DNA methylation of *PTPRG* is shown to impact PTPRG expression, and PTPRG function is shown to inhibit RAS signaling through ERK phosphorylation. The function of PTPRG as a RAS suppressor provides a novel and new target for therapy in RAS-associated leukemia, and links an epigenetic modification with a well-known genetic mutation.

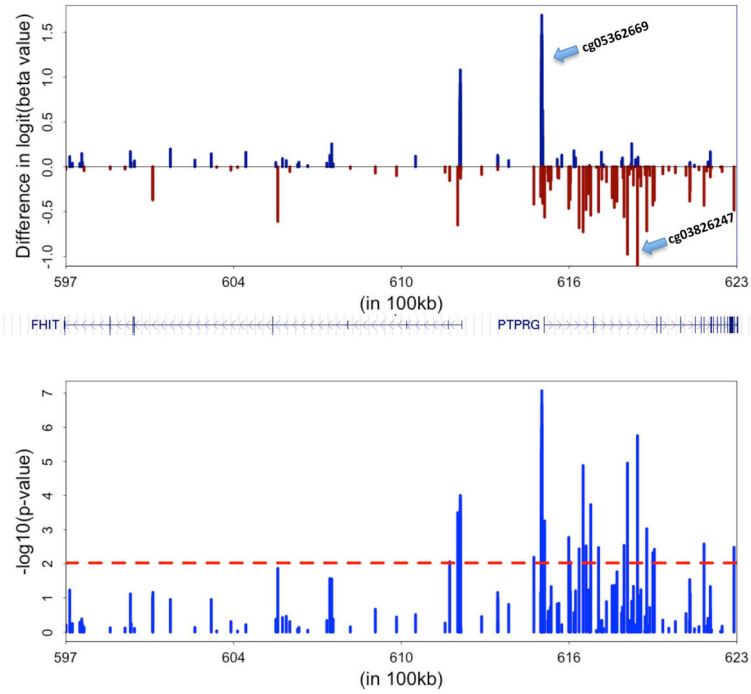

Figure 1. Association of CpG methylation in *FHIT* and *PTPRG* genes with *RAS* status

Mean differences in DNA methylation beta values between *RAS* mutant and *RAS* wild type for each CpG site within *FHIT* and *PTPRG* regions is shown in the top panel. The $-\text{Log}_{10}$(Pvalue) is shown for the comparison of DNA methylation status [Student's t-test of arcsine(beta values)] between *RAS* mutant positive patients versus negative are shown in the lower panel. The locations of CpG sites in relation to chromosome 3 location (hg19) and gene annotation is noted. Data is derived from Illumina HM450K methylation screening of 166 patients.

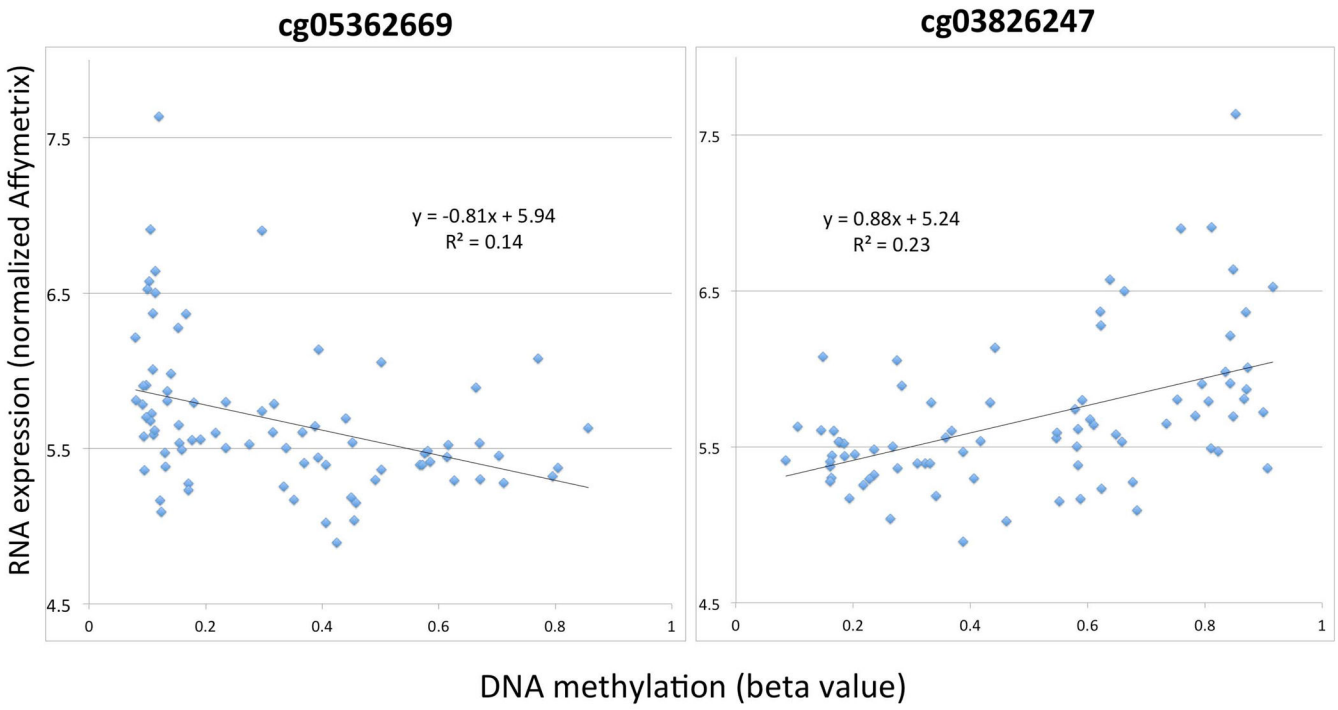

Figure 2. Relationship between methylation levels of the two top CpG loci (by P-value, for *RAS* mutations and *PTPRG* DNA methylation) and gene expression of *PTPRG*

Eighty-seven leukemia bone marrow samples were assayed with the Affymetrix ST 1.0 expression microarray as well as Illumina HM450 DNA methylation array. The DNA methylation status of the indicated Illumina loci (x-axis) were graphed against the expression of the gene (y-axis). A regression line was graphed, and the line equation and Pearson R^2 is indicated.

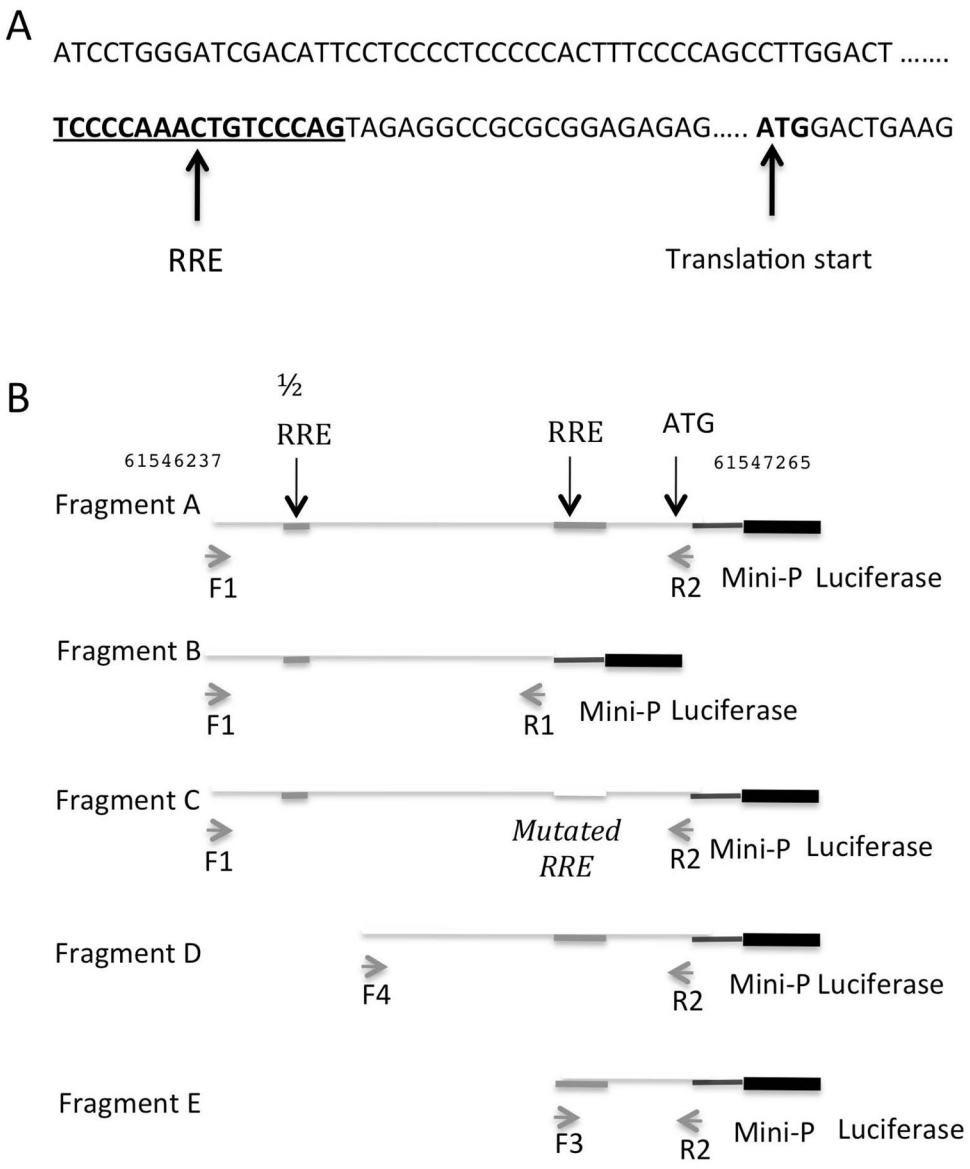

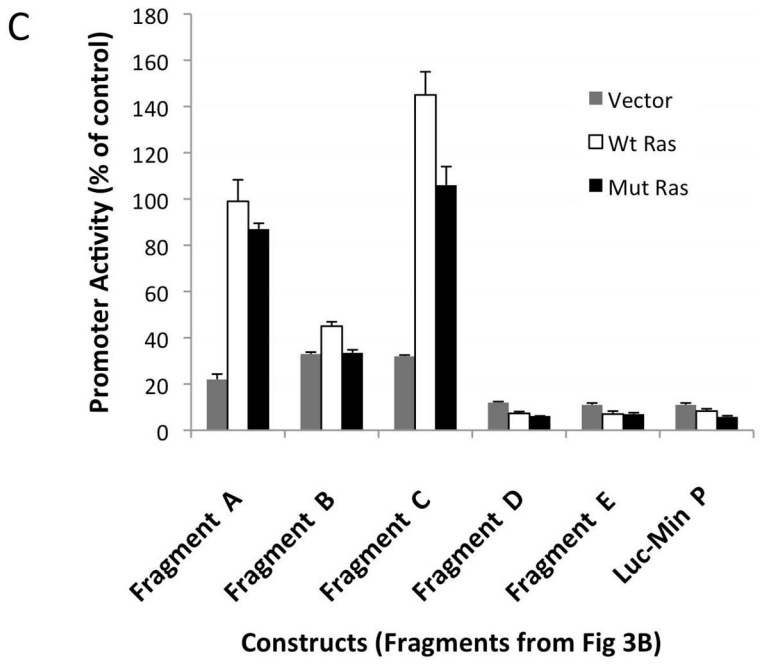

Figure 3. RRE sequences in the *PTPRG* promoter and cloning of different promoter fragments

A. A portion of the *PTPRG* promoter fragment showing a Putative RRE (bold and underlined) in the *PTPRG* promoter 290 base pairs upstream of the ATG translation start. ***B***. Cloning of the 5 different promoter fragments into the luciferase reporter plasmid. Fragment A, the full length promoter; Fragment B, the promoter lacking the RRE; Fragment C, the full length promoter with a mutated RRE (see Materials and Methods); Fragment D, short promoter containing only the RRE and its flanking sequences; Fragment E, fragment D minus the RRE and its upstream flanking sequence. ***C***. Promoter activity of the *PTPRG* promoter fragments. Promoter activity was detected using the luciferase reporter system in 293 cells. Each of the 5 different fragments and the Luc-Min P plasmid was co-transfected into 293 cells with the plasmid vector, pMSCV/neo (Vector), pMSCV/Ras Wt (Wt Ras), and pMSCV/Ras Mut (Mut Ras) respectively. Luciferase activity (y-axis) was measured as described in Materials and Methods.

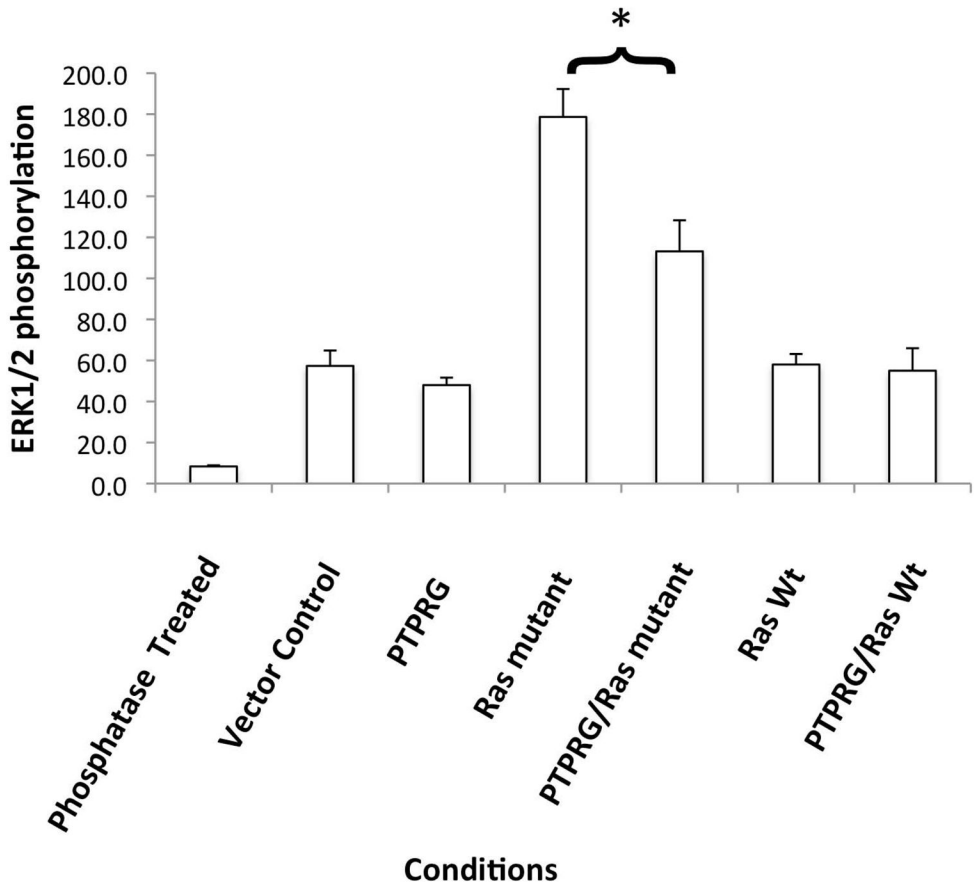

Figure 4. Inhibition of ERK1/2 phosphorylation by PTPRG

Phosphorylated ERK1/2 protein in 293 cells transfected with different plasmids was individually detected using the Bio-Plex Phospho 5-plex panel kit. Phosphorylated proteins were quantitated using the Bio-plex 200 Luminex apparatus and are expressed as fluorescence intensity. Commercial phosphatase-treated Hela cell lysates were used as a negative control. Transfection Conditions in 293 cells are the following: Vector control, the empty vector pMSCVneo; PTPRG, plasmid pMSCV/PTPRG which expresses the human *PTPRG* gene; RAS Mutant, plasmid pMSCV/RAS Mut which expresses the KRAS mutant gene; RAS Wt, plasmid pMSCV/RAS Wt which expresses the Wt KRAS gene; PTPRG/RAS Mutant, co-transfection of pMSCV/PTPRG and pMSCV/RAS Mut; PTPRG/RAS Wt, co-transfection of pMSCV/PTPRG and pMSCV/RAS Wt. Error bars indicate standard deviations. “*”, P-value was calculated using the Student T test for RAS mutant and PTPRG/RAS Mutant ($P < 0.001$).

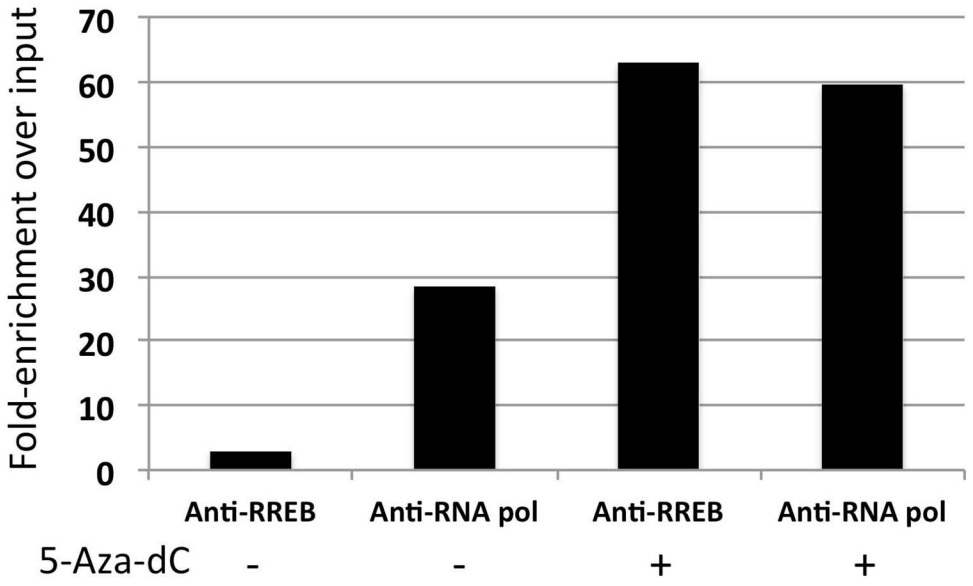

Figure 5. Chromatin Immunoprecipitation of RREB1 in cell line 697

RREB1 was immunoprecipitated from chromatin prepared from 697 cells treated with Azacytidine or buffer (+, − as noted). All bars represent an average of four experiments, and the fold-enrichment determined by quantitative PCR over the input is noted.

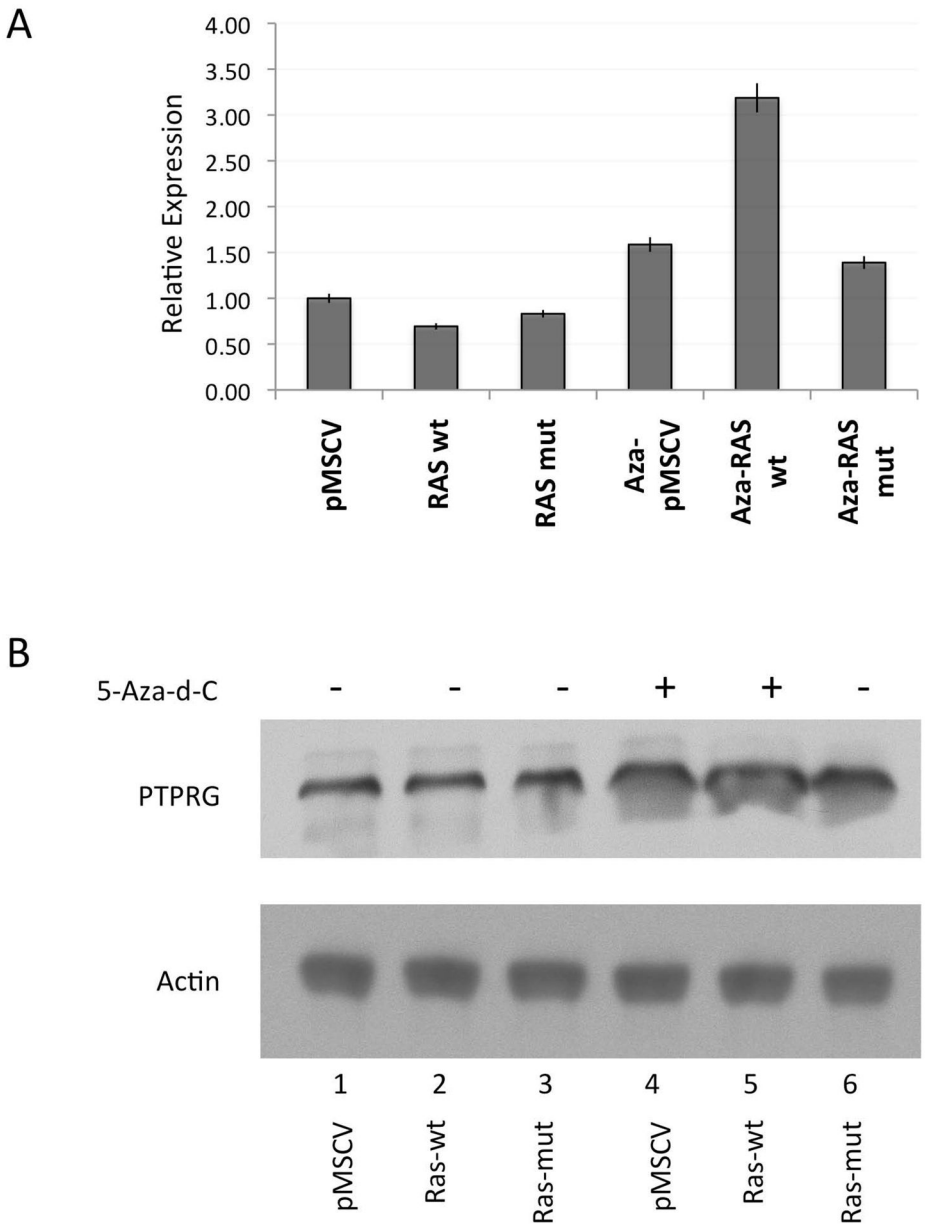

Figure 6. *PTPRG* expression in response to DNA demethylation and KRAS expression

293 cells were treated with 5-Aza-d-C, or DMSO and transfected with either the marker plasmid, pMSCV/neo, or the plasmid expressing the wt KRAS, pMSCV/RAS Wt. mRNA expression was detected by quantitative real-time RT-PCR and protein expression was detected by Western blotting. ***A.*** relative expression of PTPRG detected by Quantitative real-time RT-PCR. Error bars indicate standard deviations. PMSCV, 293 cells transfected with the marker plasmid, pMSCV/neo; RAS, 293 cells transfected with pMSCV/RAS Wt, or RAS mut, as indicated; Aza-pMSSCV, 293 cells treated with 5-Aza-d-C and transfected with pMSCV/neo; Aza-Ras Wt; 293 cells treated with 5-Aza-d-C and transfected with pMCV/RAS Wt; Aza-Ras, 293 cells treated with 5-Aza-d-C and transfected with pMCV/RAS Mut. ***B***. Western blot analysis of PTPRG protein, with the same sample order

as in A. The PTPRG and actin protein bands are indicated by the arrows, actin was detected together with PTPRG to show equal loading.

Table 1

Parameter estimates from multivariate linear regression models assessing PTPRG methylation at two CpG sites*

	Model 1		Model 2		Model 3		Model 4		Model 5	
	Parameter (SE)*	p	Parameter (SE)*	p	Parameter (SE)*	p	Parameter (SE)*	p	Parameter (SE)*	p
cg05362669										
	n** = 172		n** = 224		n** = 161		n** = 224		n** = 161	
Intercept	0.26(0.018)	<.0001	0.2309(0.0165)	<.0001	0.2086(0.0187)	<.0001	0.2657(0.0214)	<.0001	0.2469(0.0236)	<.0001
RAS	0.21(0.041)	<.0001			0.1271(0.0395)	0.0016			0.1162(0.0391)	0.0034
Hyperdiploidy			0.2011(0.0279)	<.0001	0.2187(0.0318)	<.0001	0.1663(0.0309)	<.0001	0.1842(0.0340)	<.0001
t(12;21)							−0.0833(0.0330)	0.0124	−0.0967(0.0373)	0.0105
cg03826247										
	n** = 168		n** = 219		n** = 157		n** = 219		n** = 157	
Intercept	0.55(0.020)	<.0001	0.6100(0.0177)	<.0001	0.6235(0.0205)	<.0001	0.5465(0.0224)	<.0001	0.5585(0.0253)	<.0001
RAS	−0.011	<.0001			−0.1070(0.0431)	0.0142			−0.0881(0.0414)	0.0349
Hyperdiploidy			−0.2618(0.0302)	<.0001	−0.2740(0.0351)	<.0001	−0.1983(0.0325)	<.0001	−0.2159(0.0364)	<.0001
t(12;21)							0.1500(0.0344)	<.0001	0.1606(0.0395)	<.0001

* Parameter: regression coefficient; SE: standard error. The two sites include the most significant gene promoter and gene body CpG for PTPRG association with RAS status.

** n: number of childhood ALL patients included in each analysis, which varied due to missing data.